Weak gravitational lensing and the Euclid space mission

Martin Kilbinger

CEA Saclay, Irfu/DAp - AIM, CosmoStat; IAP

École polytechnique, enseignement d'approfondissement
1 octobre 2019

martin.kilbinger@cea.fr
www.cosmostat.org/kilbinger
Slides: http://www.cosmostat.org/people/kilbinger
@energie_sombre

Overview

Books, Reviews and Lecture Notes

- Kochanek, Schneider & Wambsganss 2004, book (Saas Fee) Gravitational lensing: Strong, weak & micro. Download Part I (Introduction) and Part III (Weak lensing) from my homepage `http://www.cosmostat.org/people/kilbinger`.

- Kilbinger 2015, review Cosmology from cosmic shear observations Reports on Progress in Physics, 78, 086901, arXiv:1411.0155

- Mandelbaum 2018, review Weak lensing for precision cosmology, ARAA submitted, arXiv:1710.03235

- Sarah Bridle 2014, lecture videos (Saas Fee) `http://archiveweb.epfl.ch/saasfee2014.epfl.ch/page-110036-en.html`

Cosmology: The science of the Universe

Matter-energy content
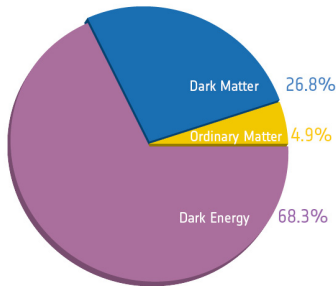
(+ photons, neutrinos)
[Planck Collaboration, 2018]

Expansion history
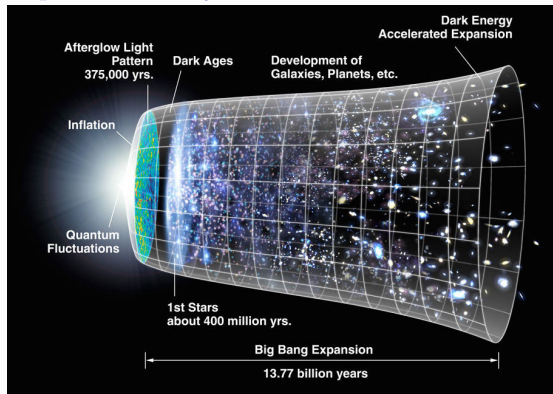
"Standard model": Flat ΛCDM cosmology.

Cosmology: The science of the Universe

Structure formation
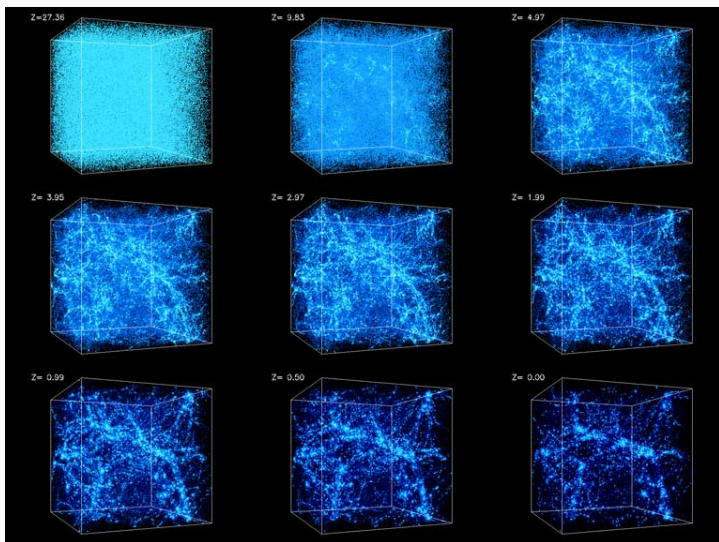
Galaxies and dark matter; (Springel et al. 2005), 10^{10} simulated particles
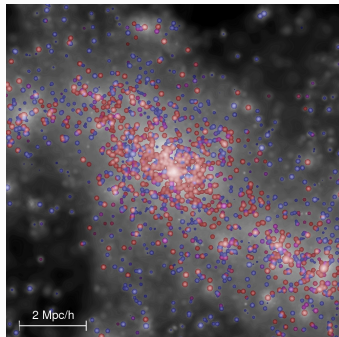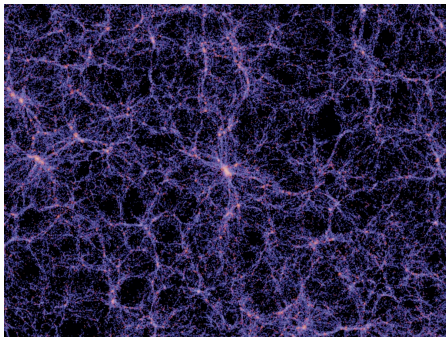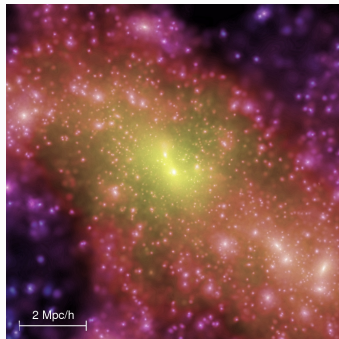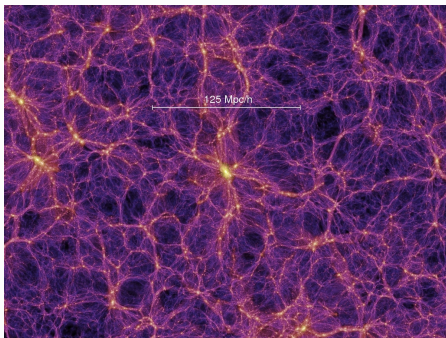
Dark matter

Indirect detection
Example: galaxy rotation curves.
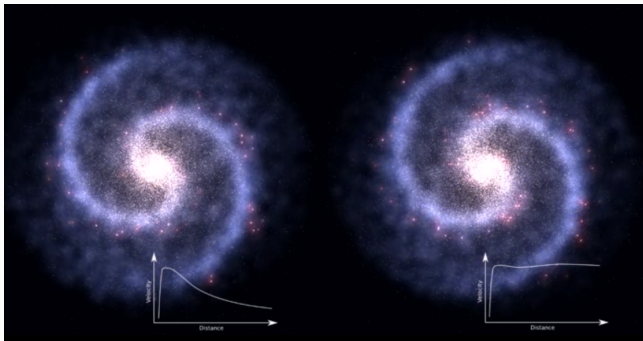
Also gravitational lensing.

Direct detection
Large under-ground experiments, no detection so far.

Dark energy

Indirect detection: Supernovae type Ia = "standard candles"
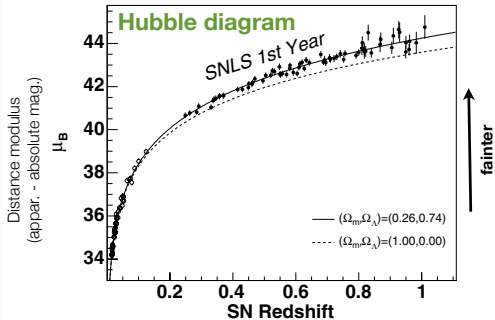
SNIa = "standard candles", absolute luminosity (more or less) fixed, relative luminosity (magnitude) only depends on distance.

Dark energy
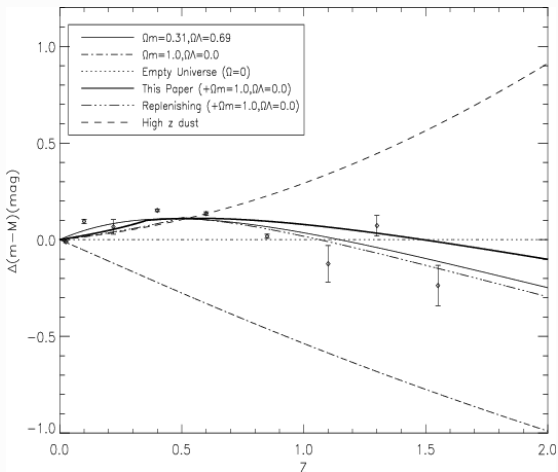
SNIa fainter than for matter-only universe at medium redshift z;
But seems to follow matter-dominated law at high z, too bright for dust
absorption of light.

Nature of dark energy?

Einstein equations:

$$R_{\mu\nu} - \frac{1}{2} g_{\mu\nu} R = \frac{8\pi G}{c^2} T_{\mu\nu} - \Lambda g_{\mu\nu}.$$

Possible interpretations:

- Λ: integration constant (cosmological constant), most general (covariant) expansion of Einstein's original equation
 Problem: Why is Λ so small, dominant today? Required fine-tuning in early universe. No explained from particle physics.

- $\Lambda g_{\mu\nu}$ as part of matter-energy tensor $T_{\mu\nu}$. Simplest case isotropic "fluid", $T_{\mu\nu} = \mathrm{diag}(\rho c^2, p, p, p)$. With $g_{\mu\nu} = \eta_{\mu\nu} = \mathrm{diag}(1, -1, -1, -1)$
  $\rightarrow p = -\rho c^2$, vacuum energy.
  Problem: Naive prediction wrong by 10^{120}!

Nature of dark energy?

Einstein equations:

$$R_{\mu\nu} - \frac{1}{2}g_{\mu\nu}R = \frac{8\pi G}{c^2}T_{\mu\nu} - \Lambda g_{\mu\nu}.$$

Possible interpretations:

- Dynamical dark energy (quintessence, K-essence, ...). Add time-dependence; add parameter w for equation of state: $p = w\rho c^2$. Holy grail of cosmology: Find $w \neq -1$, or $w(z)$! Problem: Still need fine-tuning.

- Move $\Lambda g_{\mu\nu}$ to left-hand side. Modification of Einstein's equation, modified gravity. Problem: Models not well constrained, some require fine-tuning. GR satisfied on very small and very large scales.

Gravitational lensing

Gravitational lensing = light deflection and focusing by matter

Light is deflected by both dark and luminous matter.

Important to study dark matter:

- Dominant over luminous (baryonic) matter (27% vs. 5%)
- Dark matter easy to understand and simulate (N-body simulations), only interaction is gravity

We will be looking at the small distortion of distant galaxies by the cosmic web (weak cosmological lensing, cosmic shear).
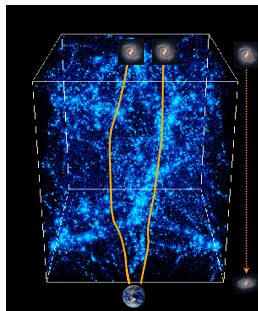
Brief history of gravitational lensing

- Before Einstein: Masses deflect photons, treated as point masses.
- 1915 Einstein's GR predicted deflection of stars by sun, deflection larger by 2 compared to classical value. Confirmed 1919 by Eddington and others during solar eclipse.
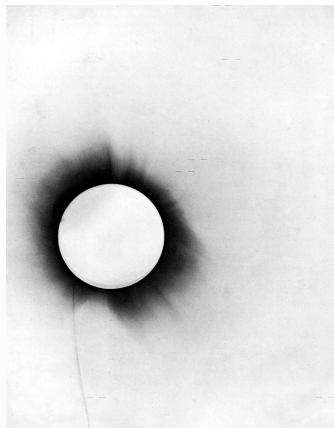
Photograph taken by Eddington of solar corona, and stars marked with bars.

Lensing on cosmological scales

- 1979 Walsh et al. detect first double image of a lenses quasar.
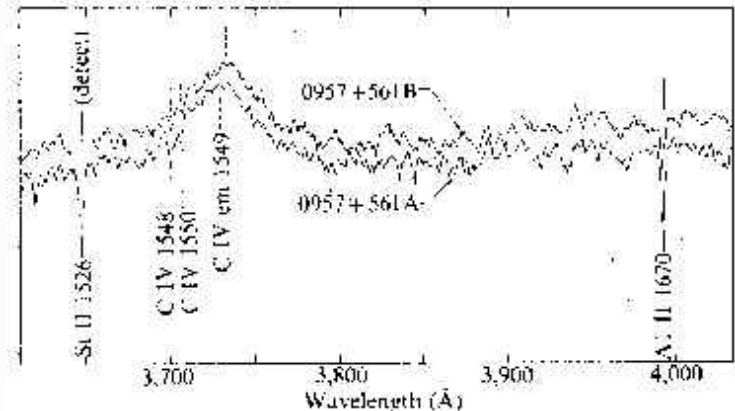
(Walsh et al. 1979)

- 1987 Soucail et al. strongly distorted "arcs" of background galaxies behind galaxy cluster, using CCDs.
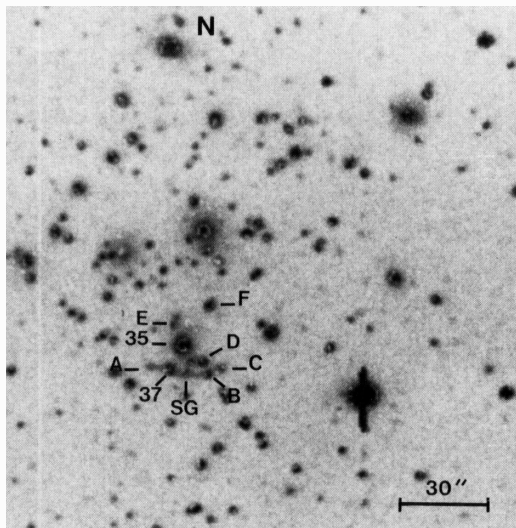
exclude that it is an off-chance superimposition of
faint cluster galaxies even if a diffuse component
seems quite clear from the R CCD field. A
gravitational lens effect on a background quasar is a
possibility owing to the curvature of the structure
but in fact it is too small (Hammer 86) and no blue
object opposite the central galaxy has been detected.
It is more likely that we are dealing with a star
formation region located in the very rich core where

- Tyson et al. (1990), tangential alignment around clusters.
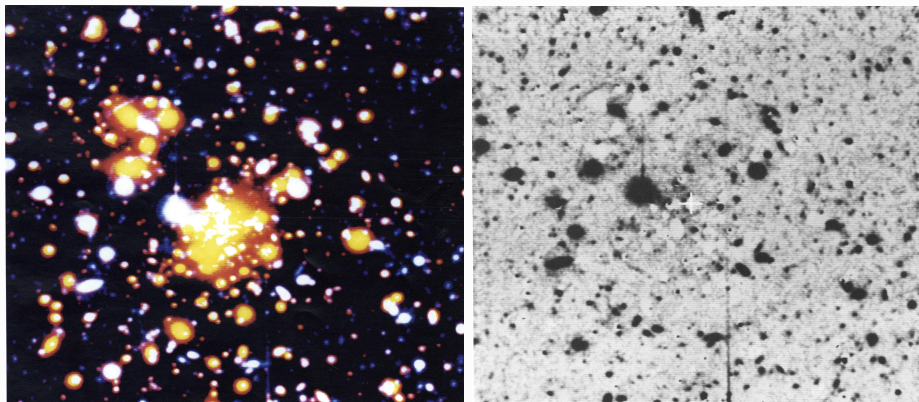
Abell 1689
Cluster outskirts: Weak gravitational lensing.

- 2000 cosmic shear: weak lensing in blind fields, by 4 groups (Edinburgh, Hawai'i, Paris, Bell Labs/US).
  Some $10,000$ galaxies on an area of a few square degrees on the sky.

- By 2018: Many dedicated surveys: DLS, CFHTLenS, DES, KiDS, HSC. Competitive constraints on cosmology.
  Factor 100 increase: Millions of galaxies over 100s of degrees. Many other improvements: Multi-band observations, photometric redshifts, image and N-body simulations, ...

- By 2025: LSST, WFIRST-AFTA, Euclid data will be available.
  Another factor of 100 increase: Hundred millions of galaxies, tens of thousands of degrees area (most of the extragalactic sky).

Light deflection

Simplest case: point mass deflects light

Deflection angle for a point mass M is

$$\hat{\alpha} = \frac{4GM}{c^2 \xi} = \frac{2R_S}{\xi}$$

R_S is the Schwarzschild radius.
(Einstein 1915)

This is twice the value one would get in a classical, Newtonian calculation.

Deflection angle: general case

source S

$\hat{\alpha}$

$\overrightarrow{\nabla_{\perp}\phi}$

observer O
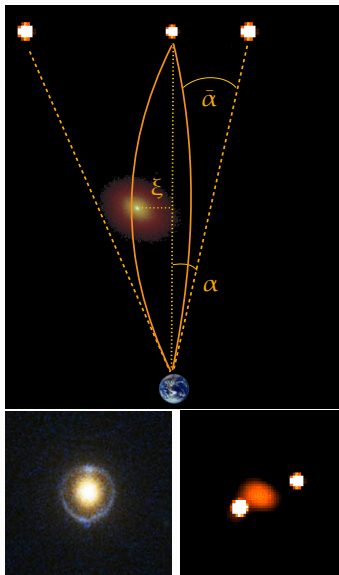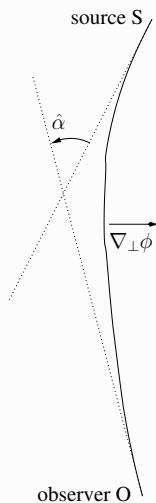
Perturbed Minkowski metric, weak-field ($\phi \ll c^2$)

$$\mathrm{d}s^2 = \left(1 + 2\phi/c^2\right) c^2 \mathrm{d}t^2 - \left(1 - 2\phi/c^2\right) \mathrm{d}\ell^2$$

One way to derive deflection angle: Fermat's principle of least light travel time.

Light travels on geodesics, $\mathrm{d}s^2 = 0$
$\rightarrow$ light travel time t is

$$t = \frac{1}{c} \int_{\mathrm{path}} \left(1 - 2\phi/c^2\right) \mathrm{d}\ell$$

Deflection angle: general case

Fermat's principle: Minimize light travel time.

Analogous to refraction in medium with refractive index $n > 1$,

$$t = \frac{1}{c} \int_{\text{path}} \left(1 - 2\phi/c^2\right) \mathrm{d}\ell = \frac{1}{c} \int_{\text{path}} n(\boldsymbol{x}) \mathrm{d}\ell$$
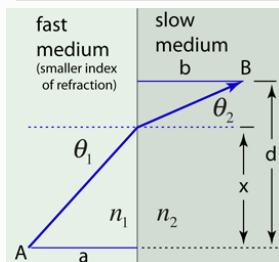
Minimize t to derive Snell's law, $\sin \theta_1 / \sin \theta_2 = n_2/n_1$.

Assume t is stationary, $\delta t = 0$.

Integrate Euler-Lagrange equations along the light path to get

$$\text{deflection angle} \qquad \hat{\boldsymbol{\alpha}} = -\frac{2}{c^2} \int_{\text{S}}^{\text{O}} \boldsymbol{\nabla}_\perp \phi \, \mathrm{d}\ell$$

Exercise: Derive the deflection angle for a point mass. I

Derive $\hat{\alpha} = 4GM/(c^2\xi)$.

We can approximate the potential as

$$\phi = -\frac{GM}{R} = -\frac{c^2}{2}\frac{R_{\rm S}}{R},$$

where G is Newton's constant, M the mass of the object, R the distance, and $R_{\rm S}$ the Schwarzschild radius

The distance R can be written as

$$R^2 = x^2 + y^2 + z^2.$$

(Weak-field condition $\phi \ll c^2$ implies $R \gg R_{\rm S}$.)
(Here z is not redshift, but radial (comoving) distance.)

We use the so-called Born approximation (from quantum mechanic scattering theory) to integrate along the unperturbed light ray, which is a straight line parallel to the z-axis with a constant $x^2 + y^2 = \xi^2$. The impact parameter ξ is the distance of the light ray to the point mass.

Exercise: Derive the deflection angle for a point mass. II

The deflection angle is then

$$\hat{\boldsymbol{\alpha}} = -\frac{2}{c^2} \int_{-\infty}^{\infty} \boldsymbol{\nabla}_{\perp} \phi \, \mathrm{d}z.$$

The perpendicular gradient of the potential is

$$\boldsymbol{\nabla}_{\perp} \phi = \frac{c^2 R_{\mathrm{S}}}{2|R|^3} \left(\begin{array}{c} x \\ y \end{array} \right) = \frac{c^2 R_{\mathrm{S}}}{2} \frac{\xi}{(\xi^2 + z^2)^{3/2}} \left(\begin{array}{c} \cos\varphi \\ \sin\varphi \end{array} \right).$$

The primitive for $(\xi^2 + z^2)^{-3/2}$ is $z\xi^{-2}(\xi^2 + z^2)^{-1/2}]$. We get for the absolute value of the deflection angle

$$\hat{\alpha} = R_{\mathrm{S}} \left[\frac{z}{\xi(\xi^2 + z^2)^{1/2}} \right]_{-\infty}^{\infty} = \frac{R_{\mathrm{S}}}{\xi} \left[1 - (-1) \right] = \frac{2R_{\mathrm{S}}}{\xi} = \frac{4GM}{c^2 \xi}.$$

Generalisation I: mass distribution I

Distribution of point masses $M_i(\boldsymbol{\xi}_i, z)$: total deflection angle is linear vectorial sum over individual deflections

$$\hat{\boldsymbol{\alpha}}(\boldsymbol{\xi}) = \sum_i \delta\hat{\boldsymbol{\alpha}}(\boldsymbol{\xi} - \boldsymbol{\xi}_i) = \frac{4G}{c^2} \sum_i \delta M_i(\boldsymbol{\xi}_i, z_i) \frac{\boldsymbol{\xi} - \boldsymbol{\xi}_i}{|\boldsymbol{\xi} - \boldsymbol{\xi}_i|^2}$$

A small mass is related to a volume element via the density, $\delta M = \rho \delta V$. Perform transition to continuous density

$$\sum_i \delta M_i \rightarrow \int \mathrm{d}M = \int \rho(\boldsymbol{x}) \mathrm{d}^3 x = \int \mathrm{d}^2 \xi' \int \mathrm{d}z' \, \rho(\boldsymbol{\xi}', z')$$

and introduction of the 2D

$$\text{surface mass density} \quad \Sigma(\boldsymbol{\xi}') = \int \mathrm{d}z' \, \rho(\boldsymbol{\xi}', z')$$

we get

$$\hat{\boldsymbol{\alpha}}(\boldsymbol{\xi}) = \frac{4G}{c^2} \int \mathrm{d}^2 \xi' \, \Sigma(\boldsymbol{\xi}') \frac{\boldsymbol{\xi} - \boldsymbol{\xi}'}{|\boldsymbol{\xi} - \boldsymbol{\xi}'|^2}$$

Thin-lens approximation

Generalisation I: mass distribution II

Gravitational lensing Can probe complex mass profiles ρ, or (2D projected) Σ.
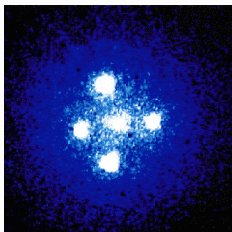
"Einstein cross", $z_\mathrm{s} = 1.7, z_\mathrm{l} = 0.04$

WFI2033-4723, $z_\mathrm{s} = 1.66, z_\mathrm{l} = 0.66$
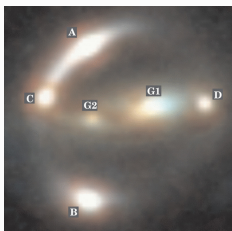
CLASS B1608+656, $z_\mathrm{s} = 1.394, z_\mathrm{l} = 0.63$.
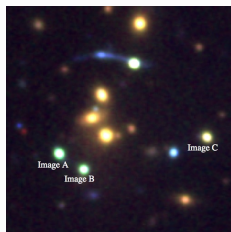
SDSS J2222+2745, $z_\mathrm{s} = 2.82, z_\mathrm{l} = 0.49$.

Generalisation II: Extended source

Extended source: different light rays impact lens at different positions $\boldsymbol{\xi}$, their deflection angle $\boldsymbol{\alpha}(\boldsymbol{\xi})$ will be different: differential deflection $\rightarrow$ distortion, magnification of source image!

The cluster of galaxies Abell 2218
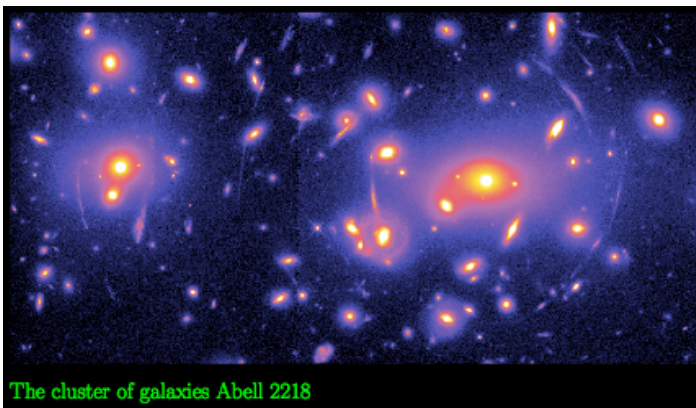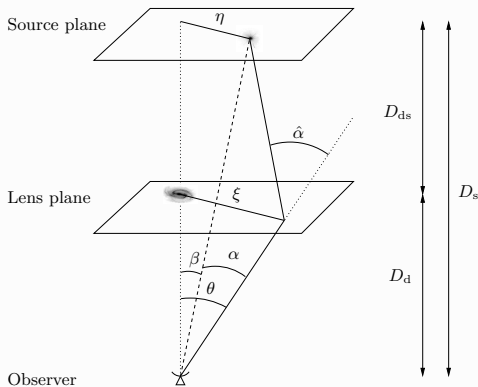
Lens equation

Defining rescaled deflection angle $\boldsymbol{\alpha} = \frac{D_{ds}}{D_s}\hat{\boldsymbol{\alpha}}$.

The simple equation relating lens to source extend is called lens equation

$$\boldsymbol{\beta} = \boldsymbol{\theta} - \boldsymbol{\alpha}(\theta).$$

This is a mapping from lens coordinates $\boldsymbol{\theta}$ to source coordinates $\boldsymbol{\beta}$. Why?

Cosmic shear: continuous deflection along line of sight
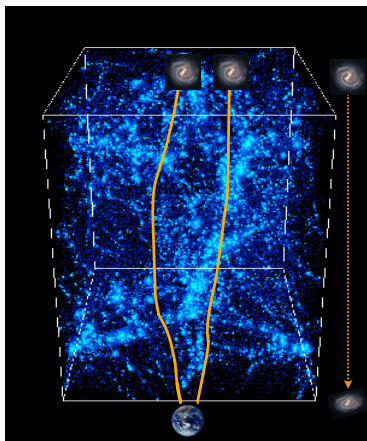
With the Born approximations, and assumption that structures along line of sight are un-correlated:

Deflection angle can be written as gradient of a potential, called lensing potential ψ:

$$\alpha(\boldsymbol{\theta}) = \boldsymbol{\nabla}\psi(\boldsymbol{\theta})$$

$$\psi(\boldsymbol{\theta}) = \frac{2}{c^2} \int_0^\chi \mathrm{d}\chi' \frac{\chi - \chi'}{\chi\chi'}\, \Phi(\chi'\boldsymbol{\theta}, \chi').$$

for a source at comoving distance χ.

Note: Difference between Born and actual light path up to few Mpc!

Linearizing the lens equation

We talked about differential deflection before. To first order, this involves the derivative of the deflection angle.

$$\frac{\partial \beta_i}{\partial \theta_j} \equiv A_{ij} = \delta_{ij} - \partial_j \alpha_i = \delta_{ij} - \partial_i \partial_j \psi.$$

Jacobi (symmetric) matrix

$$A = \begin{pmatrix} 1 - \kappa - \gamma_1 & -\gamma_2 \\ -\gamma_2 & 1 - \kappa + \gamma_1 \end{pmatrix}.$$

- convergence κ: isotropic magnification
- shear γ: anisotropic stretching
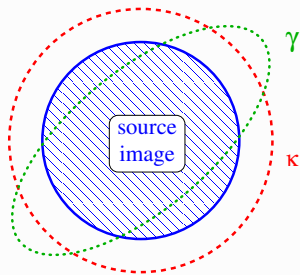
Convergence and shear are second derivatives of the 2D lensing potential.

Convergence and shear I

The effect of κ and γ follows from Liouville's theorem: Surface brightness is conserved (no photon gets lost).

We see that shear transforms a circular image into an elliptical one.

Define complex shear

$$\gamma = \gamma_1 + \mathrm{i}\gamma_2 = |\gamma|\mathrm{e}^{2\mathrm{i}\varphi};$$

The relation between convergence, shear, and the axis ratio of elliptical isophotes is then

$$|\gamma| = |1 - \kappa|\frac{1 - b/a}{1 + b/a}$$
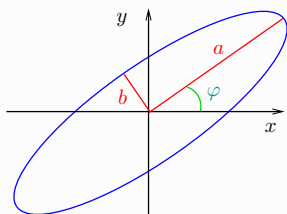
Convergence and shear II

Further consequence of lensing: magnification.
Liouville (surface brightness is conserved) + area changes ($d\beta^2 \neq d\theta^2$ in general) $\rightarrow$ flux changes.

$$\text{magnification} \quad \mu = \det A^{-1} = [(1-\kappa)^2 - \gamma^2]^{-1}.$$

Magnification important to account for by other cosmological probes:
Changes population of objects (selection effects), magnitude of standard candles (SNe Ia), standard sirens (GWs), galaxy clustering amplitude.

Summary: Convergence and shear linearly encompass information about projected mass distribution (lensing potential ψ). They quantify how lensed images are magnified, enlarged, and stretched. These are the main observables in (weak) lensing.

Effects of lensing, $\partial^i \psi / \partial x^i$

i	symbol	name	spin	effect	
0	Δt	time delay	0		
1	α	deflection	1		
2	κ	convergence	0		
2	γ	shear	2		
3	F	flexion	1		
3	G	flexion	3		
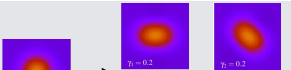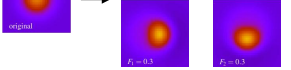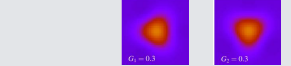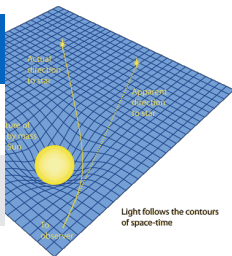
image credit Massimo Meneghetti

shear + flexion

$-\gamma_1 + G_1$

Convergence and cosmic density contrast

Back to the lensing potential

- Since $\kappa = \frac{1}{2}\Delta\psi$:

$$\kappa(\boldsymbol{\theta}, \chi) = \frac{1}{c^2} \int_0^\chi \mathrm{d}\chi' \frac{(\chi - \chi')\chi'}{\chi} \Delta_{\boldsymbol{\theta}} \Phi(\chi'\boldsymbol{\theta}, \chi')$$

- Terms $\Delta_{\chi'\chi'}\phi$ average out when integrating along line of sight, can be added to yield 3D Laplacian (error $\mathcal{O}(\phi) \sim 10^{-5}$).

- Poisson equation

$$\Delta\Phi = \frac{3H_0^2\Omega_{\mathrm{m}}}{2a} \delta \qquad \left(\delta = \frac{\rho - \bar{\rho}}{\rho}\right)$$

$$\to \kappa(\boldsymbol{\theta}, \chi) = \frac{3}{2}\Omega_{\mathrm{m}} \left(\frac{H_0}{c}\right)^2 \int_0^\chi \mathrm{d}\chi' \frac{(\chi - \chi')\chi'}{\chi a(\chi')} \delta\left(\chi'\boldsymbol{\theta}, \chi'\right).$$

Convergence with source redshift distribution

So far, we looked at the convergence for one single source redshift (distance χ). Now, we calculate κ for a realistic survey with a redshift distribution of source galaxies. We integrate over the pdf $p(\chi)\mathrm{d}\chi = p(z)\mathrm{d}z$, to get

$$\kappa(\boldsymbol{\theta}) = \int\limits_0^{\chi_{\mathrm{lim}}} \mathrm{d}\chi\, p(\chi)\, \kappa(\boldsymbol{\theta}, \chi) = \int\limits_0^{\chi_{\mathrm{lim}}} \mathrm{d}\chi\, G(\chi)\, \chi\, \delta\left(\chi\boldsymbol{\theta}, \chi\right)$$

with lens efficiency

$$G(\chi) = \frac{3}{2} \left(\frac{H_0}{c}\right)^2 \frac{\Omega_{\mathrm{m}}}{a(\chi)} \int_\chi^{\chi_{\mathrm{lim}}} \mathrm{d}\chi'\, p(\chi') \frac{\chi' - \chi}{\chi'}.$$

The convergence is a projection of the matter-density contrast, weighted by the source galaxy distribution and angular distances.

Parametrization of redshift distribution, e.g.

$$p(z) \propto \left(\frac{z}{z_0} \right)^{\alpha} \exp \left[- \left(\frac{z}{z_0} \right)^{\beta} \right]$$
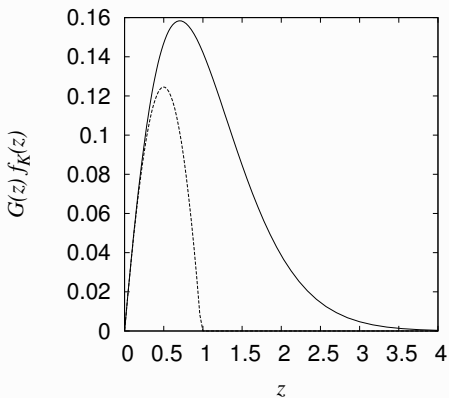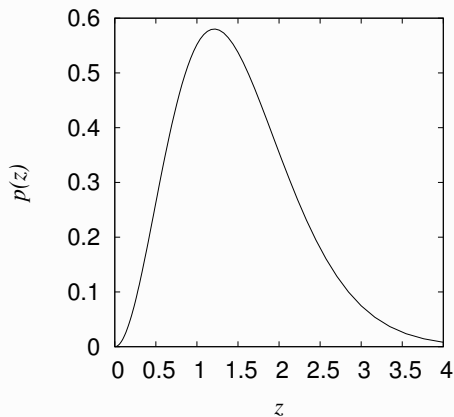
$\alpha = 2, \beta = 1.5, z_0 = 1$
(dashed line: all sources at redshift 1)

Max. lensing signal from halfway distance between us and lensing galaxies.

More on the relation between κ and γ

Convergence and shear are second derivatives of lensing potential $\rightarrow$ they are related.

One can derive κ from γ (except constant *mass sheet* κ_0).

E.g. get projected mass reconstruction of clusters from ellipticity observations.

Projected matter density
convergence κ

Distortion field
shear γ

−0.041   0.095   0.23

tangential distortions around mass peaks

overdensity
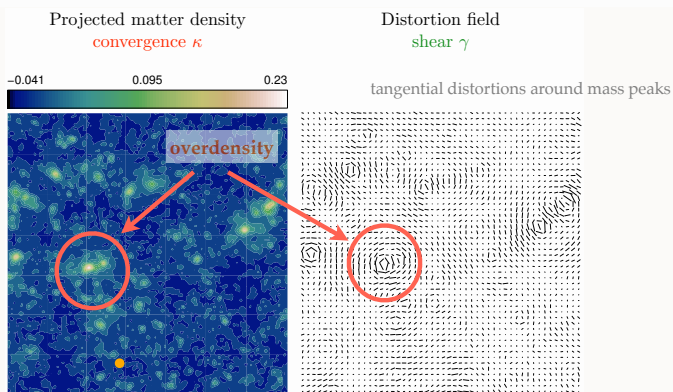
Source galaxies at $z = 1$, ray-tracing simulations by T. Hamana

Basic equation of weak lensing

Weak lensing regime

$\kappa \ll 1, |\gamma| \ll 1$.

The observed ellipticity of a galaxy is the sum of the intrinsic ellipticity and the shear:

$$\varepsilon^{\mathrm{obs}} \approx \varepsilon^{\mathrm{s}} + \gamma$$

Random intrinsic orientation of galaxies

$$\langle \varepsilon^{\mathrm{s}} \rangle = 0 \quad \longrightarrow \quad \boxed{\langle \varepsilon^{\mathrm{obs}} \rangle = \gamma}$$

The observed ellipticity is an unbiased estimator of the shear. Very noisy though! $\sigma_\varepsilon = \langle |\varepsilon^{\mathrm{s}}|^2 \rangle^{1/2} \approx 0.4 \gg \gamma \sim 0.03$. Increase S/N and beat down noise by averaging over large number of galaxies.

Question: Why is the equivalent estimation of the convergence and/or magnification more difficult?

Ellipticity and local shear
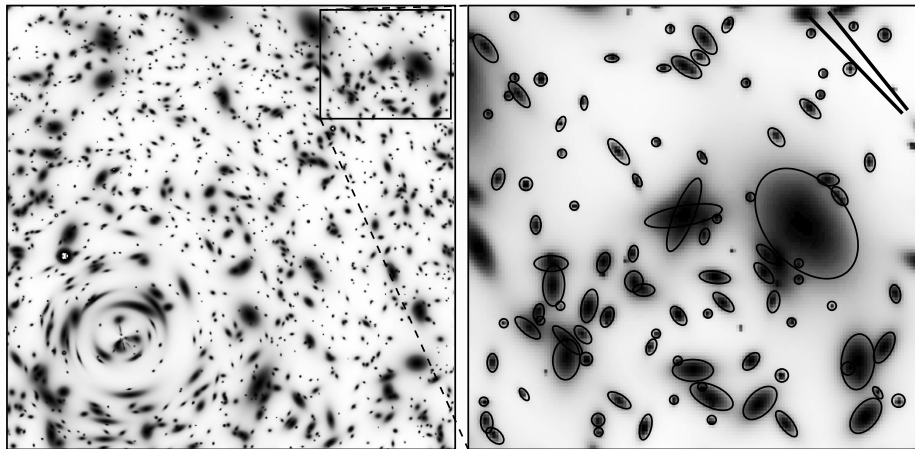
[from Y. Mellier]
Galaxy ellipticities are an estimator of the local shear.

More on the relation between κ and γ

Convergence and shear are second derivatives of lensing potential $\rightarrow$ they are related.

In particular, fluctuations (variance σ^2) in κ and γ are the same!

Source galaxies at $z = 1$, ray-tracing simulations by T. Hamana
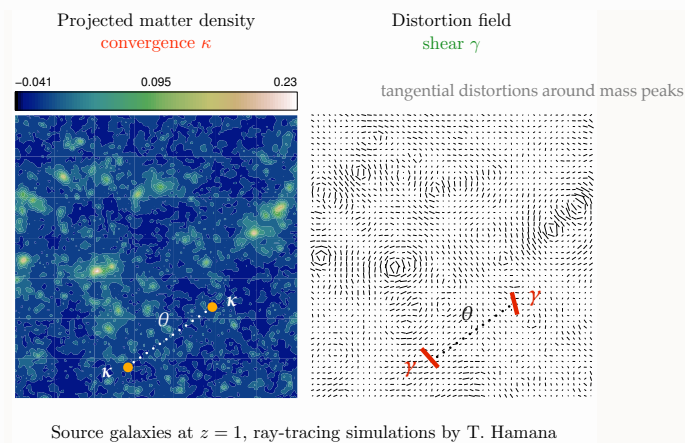
Characterising density fluctuations

Goal:

Statistical description of the large-scale structure (cosmic web).
First define density contrast

$$\delta(\boldsymbol{x}, t) = \frac{\rho(\boldsymbol{x}, t) - \bar{\rho}(t)}{\bar{\rho}(t)}.$$

By definition the expectation value (or spatial mean) vanishes

$$\langle \delta \rangle = 0,$$

since $\langle \rho \rangle = \rho$, so no (statistical) information in first moment.
$\to$ go to second moment $\langle \delta^2 \rangle$
Including spatial information: two-point correlation funtion ξ

$$\langle \delta(\boldsymbol{x}) \delta(\boldsymbol{x} + \boldsymbol{r}) \rangle_{\boldsymbol{x}} =: \xi(\boldsymbol{r})$$

For statistical isotropic (rotational invariance) and homogeneous (translational
invariance) random field δ:

$$\xi(\boldsymbol{r}) = \xi(r)$$

Characterising density fluctuations

Example: (galaxy) number density corrlelation function = excess probability
of finding an object at distance r,

$$\mathrm{d}^2 p = \bar{n}^2 \mathrm{d}V_1 \mathrm{d}V_2 \left[1 + \xi(r)\right].$$

$\xi = 0$: Poisson distribution
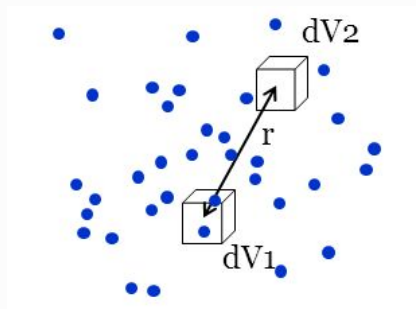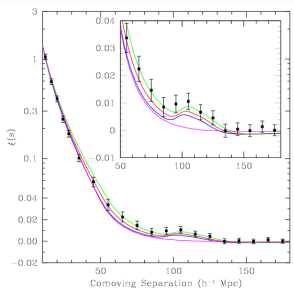
Measured galaxy correlation function,
[SDSS].

Characterising density fluctuations

Excess probability $\leftrightarrow$ more likely to find objects near other objects $\leftrightarrow$ clustering.

Clustering is a direct consequence of gravitational collapse in an expanding Universe.

Two-point correlation function only lowest-order statistic to describe field.

To quantify rich structure of voids, walls, filaments & clusters, need to go to higher-order correlations.
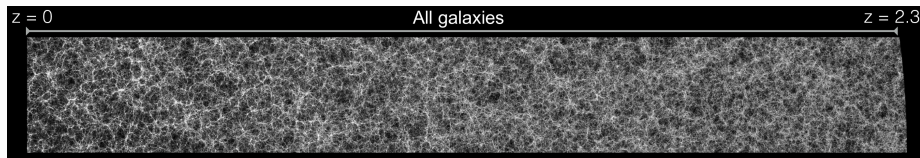
Euclid flagship simulations, (Potter et al. 2016)

The convergence power spectrum

- Variance of convergence $\langle \kappa(\boldsymbol{\vartheta} + \boldsymbol{\theta})\kappa(\boldsymbol{\vartheta})\rangle = \langle \kappa\kappa\rangle(\theta)$ depends on variance of the density contrast $\langle \delta\delta\rangle$.

- In Fourier space:

$$\langle \hat{\kappa}(\boldsymbol{\ell})\hat{\kappa}^*(\boldsymbol{\ell}')\rangle = (2\pi)^2 \delta_{\mathrm{D}}(\boldsymbol{\ell} - \boldsymbol{\ell}') P_\kappa(\ell)$$

$$\left\langle \hat{\delta}(\boldsymbol{k})\hat{\delta}^*(\boldsymbol{k}')\right\rangle = (2\pi)^3 \delta_{\mathrm{D}}(\boldsymbol{k} - \boldsymbol{k}') P_\delta(k)$$

- Limber's equation

$$P_\kappa(\ell) = \int \mathrm{d}\chi \, G^2(\chi) P_\delta\left(k = \frac{\ell}{\chi}\right)$$

  using small-angle approximation, $P_\delta(k) \approx P_\delta(k_\perp)$, contribution only from Fourier modes $\perp$ to line of sight. Also assumes that power spectrum varies slowly.

- It turns out that $\boxed{P_\kappa = P_\gamma}$
  So we use γ in observations, and κ in modelling.

Dependence on cosmology

**initial conditions,
growth of structure**

matter density

**redshift distribution
of source galaxies**

geometry

$$P_\kappa(\ell) = \int d\chi \, G^2(\chi) P_\delta \left(k = \frac{\ell}{\chi} \right)$$

$$G(\chi) = \frac{3}{2} \left(\frac{H_0}{c} \right)^2 \frac{\Omega_m}{a(\chi)} \int_\chi^{\chi_{\lim}} d\chi \, p(\chi') \frac{\chi' - \chi}{\chi'}$$

Lensing 'tomography' (2 1/2 D lensing)

- Bin galaxies in redshift.
- Lensing efficiency different for different bins: measure z-depending expansion and growth history.
- Necessary to measure dark energy, modified gravity.

comoving distance

$$P_\kappa(\ell) = \int\limits_0^{\chi_{\lim}} \mathrm{d}\chi\, G^2(\chi) P_\delta\left(k = \frac{\ell}{\chi}\right) \rightarrow$$
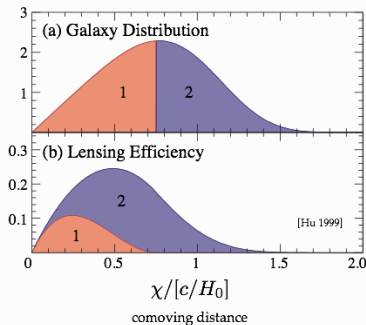
$$P_\kappa^{ij}(\ell) = \int\limits_0^{\chi_{\lim}} \mathrm{d}\chi\, G_i(\chi) G_j(\chi) P_\delta\left(k = \frac{\ell}{\chi}\right)$$

$$G_i(\chi) = \frac{3}{2}\left(\frac{H_0}{c}\right)^2 \frac{\Omega_{\mathrm{m}}}{a(\chi)} \int\limits_\chi^{\chi_{\lim}} \mathrm{d}\chi'\, p_i(\chi') \frac{\chi' - \chi}{\chi'}.$$

2019-09-27
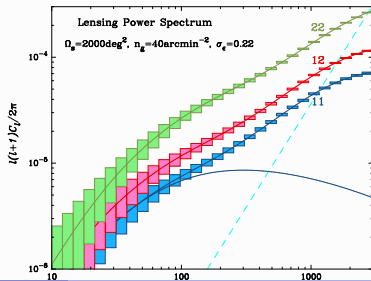
Weak lensing & Euclid
└─Basics of gravitational lensing
  └─Projected power spectrum
    └─Lensing 'tomography' (2 1/2 D lensing)
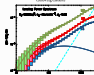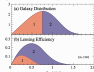
Question: Why does P_κ increase with z?

Comparison to CMB angular power spectrum

Unlike CMB C_ℓ's, features in matter power spectrum are washed out by projection and non-linear evolution.
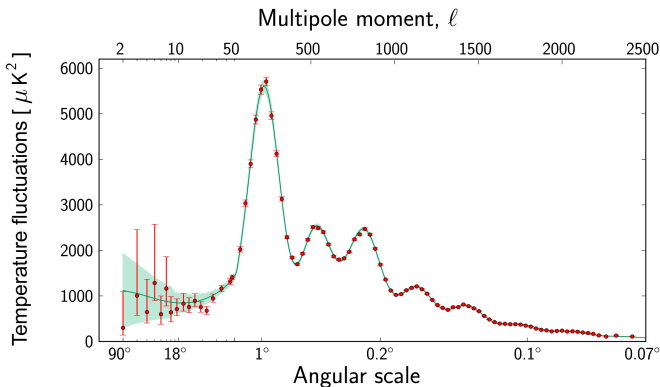
[Planck Consortium]

The shape measurement challenge

$\gamma \sim 0.03$
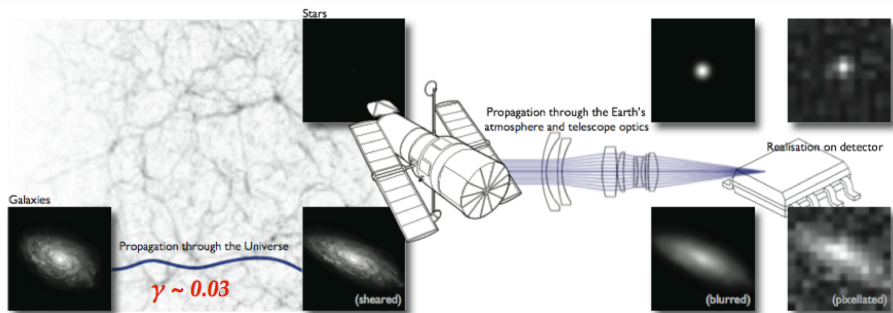
Bridle et al. 2008, great08 handbook

- Cosmological shear $\gamma \ll \varepsilon$ intrinsic ellipticity
- Galaxy images corrupted by PSF (point-spread function)
- Measured shapes are biased

Measuring cosmic shear

Typical shear of a few percent equivalent to difference in ellipticity between Uranus and the Moon.

The shape measurement challenge

How do we measure "ellipticity" for irregular, faint, noisy objects?
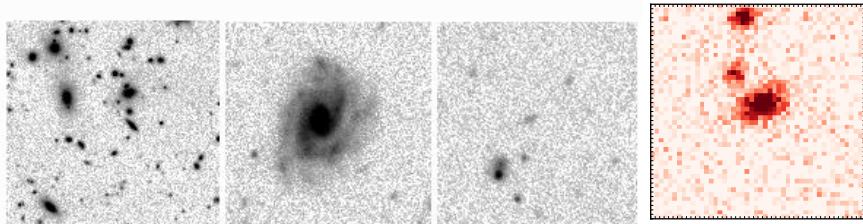
[Y. Mellier/CFHT(?)] — (Jarvis et al. 2016)
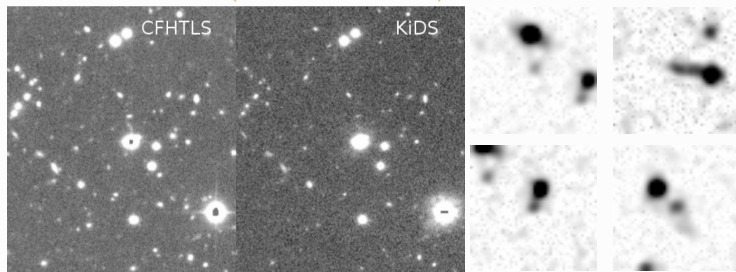
[CFHTLenS/KiDS image — CFHTlenS postage stamps]

Shape measurement

Example: Model fitting
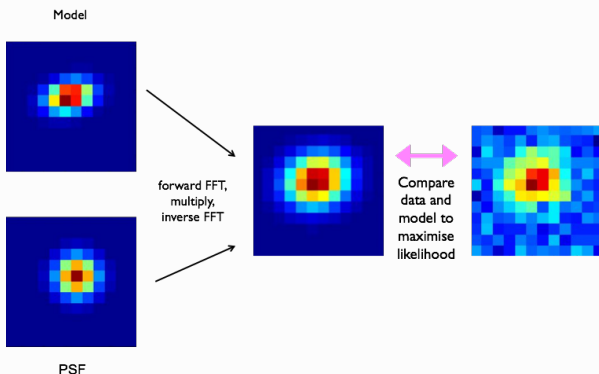
Forward model-fitting (example *lens*fit)

- Convolution of model with PSF instead of devonvolution of image
- Combine multiple exposures (in Bayesian way, multiply posterior density), avoiding co-adding of (dithered) images

Dithering
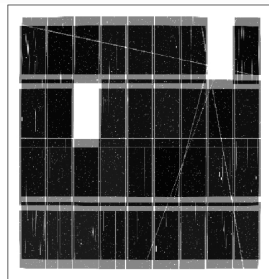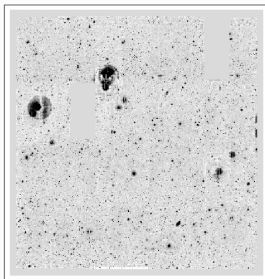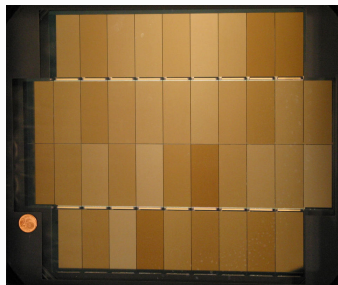
Left: Image of the MegaCam focal plane (CCDs arrays).

Middle: Co-add of two r-band exposures of CFHTLenS (without the 4 new CCDs).

Right: Weight map.

Shear measurement biases I

Origins

- **Noise bias**: In general, ellipticity is non-linear in pixel data (e.g. normalization by flux). Pixel noise $\rightarrow$ biased estimators.
- **Model bias**: Assumption about galaxy light distribution is in general wrong.
- **Other**: Imperfect PSF correction, detector effects (CTI — charge transfer inefficiency), selection effects (probab. of detection/sucessful ε measurement depends on ε and PSF)

Characterisation

Bias can be multiplicative ($\boldsymbol{m}$) and additive ($\boldsymbol{c}$):

$$\gamma_i^{\mathrm{obs}} = (1 + m)\gamma_i^{\mathrm{true}} + c; \quad i = 1, 2.$$

Biases $\boldsymbol{m}, \boldsymbol{c}$ are typically complicated functions of galaxy properties (e.g. size, magnitude, ellipticity), redshift, PSF, …. They can be scale-dependent.

Current methods: $|m| = 1\% - 10\%, |c| = 10^{-3} - 10^{-2}$.

Blind simulation challenges have been run to quantify biases, getting ideas from computer science community (e.g. http://great3challenge.info).

Weak lensing & Euclid
└─ Weak lensing measurement
  └─ Galaxy shape measurement
    └─ Shear measurement biases

Shear measurement biases I

Origins
- **Noise bias**: In general, ellipticity is non-linear in pixel data (e.g. normalization by flux). Pixel noise → biased estimators.
- **Model bias**: Assumption about galaxy light distribution is in general wrong.
- **Other**: Imperfect PSF correction, detector effects (CTI → charge transfer inefficiency), selection effects (prob. of detection/successful z measurement depends on z and PSF)

Characterisation
Bias can be multiplicative (m) and additive (c):

$$\gamma_i^{obs} = (1+m_i)\gamma_i^{true} + c_i \quad i = 1, 2.$$

Biases m, c are typically complicated functions of galaxy properties (e.g. size, magnitude, ellipticity), redshift, PSF, ... They can be scale-dependent.

Current methods: $|m| = 1\% - 10\%, |c| = 10^{-3} - 10^{-2}$.

Blind simulation challenges have been run to quantify biases, getting ideas from computer science community (e.g. http://great3challenge.info).

rgpp/rp = FWHM of PSF-convolved galaxy to PSF

Shear measurement biases II

Calibration

Using simulated or emulated data
(or self-calibration).

Functional dependence of m on
observables must not be too
complicated (e.g. not smooth,
many variables, large parameter
space), or else measurement is *not
calibratable*!
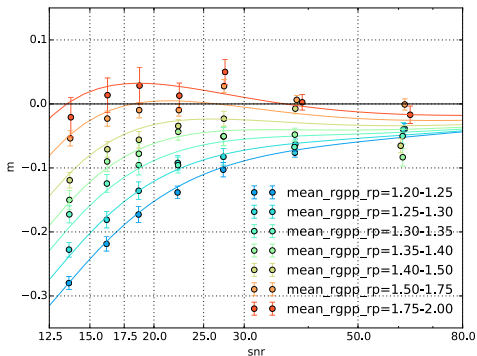
(Jarvis et al. 2016) - image simulations

Requirements for surveys
Necessary knowledge of residual biases $|\Delta m|, |\Delta c|$ (after calibration):
Current surveys 1%.
Future large missions (Euclid, LSST, ...) $10^{-4} = 0.1\%$!

Shear measurement biases III

Complex bias dependencies

Need to account for bias as function of more than one galaxy property.
E.g. size and SNR. Also need to know bulge and disc fraction of observed population.
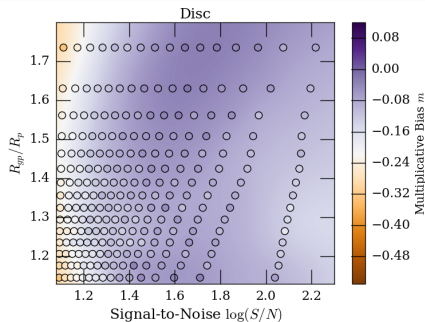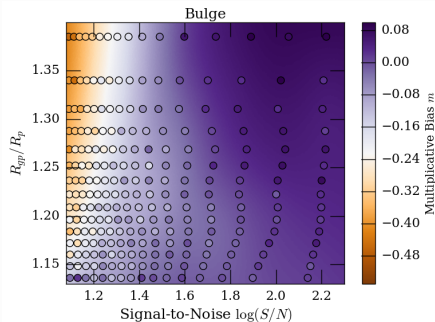

(Zuntz et al. 2018)

PSF correction

(Jarvis et al. 2016)

- Select clean sample of stars
- Measure star shapes
- Create PSF model and interpolate (pixel values, ellipticity, PCA coefficients, ...) to galaxy positions. Space-based observations: global PSF model from many exposures possible
- Correct for PSF: galaxy image devonvolution or other (e.g. linearized) correction, or convolve model

PSF correction

(Jarvis et al. 2016)

- Select clean sample of stars
- Measure star shapes
- Create PSF model and interpolate (pixel values, ellipticity, PCA coefficients, . . .) to galaxy positions. Space-based observations: global PSF model from many exposures possible
- Correct for PSF: galaxy image devonvolution or other (e.g. linearized) correction, or convolve model

PSF correction

PSF

$e = 0.01$ $e = 0.03$

PSF residual

$\delta e = 0.01$ $\delta e = 0.03$

(Jarvis et al. 2016)

- Select clean sample of stars
- Measure star shapes
- Create PSF model and interpolate (pixel values, ellipticity, PCA coefficients, . . .) to galaxy positions. Space-based observations: global PSF model from many exposures possible
- Correct for PSF: galaxy image devonvolution or other (e.g. linearized) correction, or convolve model

PSF correction

(Gentile et al. 2013)

- Select clean sample of stars
- Measure star shapes
- Create PSF model and interpolate (pixel values, ellipticity, PCA coefficients, ...) to galaxy positions. Space-based observations: global PSF model from many exposures possible
- Correct for PSF: galaxy image devonvolution or other (e.g. linearized) correction, or convolve model

PSF correction

(Gentile et al. 2013)

- Select clean sample of stars
- Measure star shapes
- Create PSF model and interpolate (pixel values, ellipticity, PCA coefficients, ...) to galaxy positions. Space-based observations: global PSF model from many exposures possible
- Correct for PSF: galaxy image devonvolution or other (e.g. linearized) correction, or convolve model

PSF interpolation
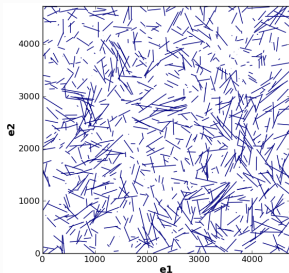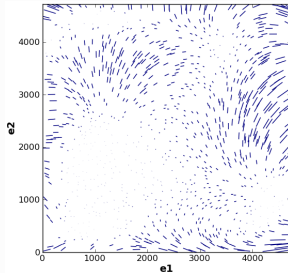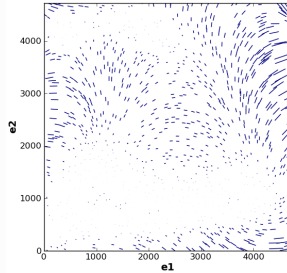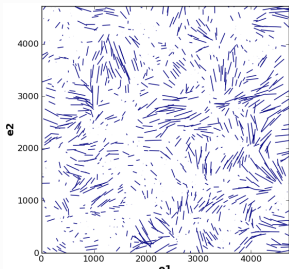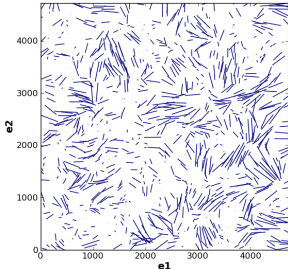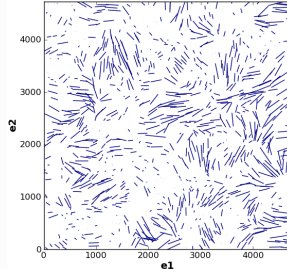
PSF model residuals, more examples
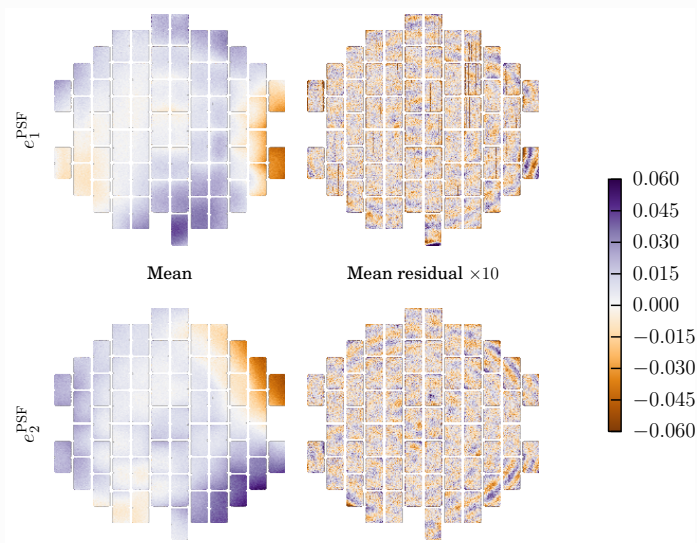
DES-Y1, (Zuntz et al. 2018)

PSF model residuals, more examples
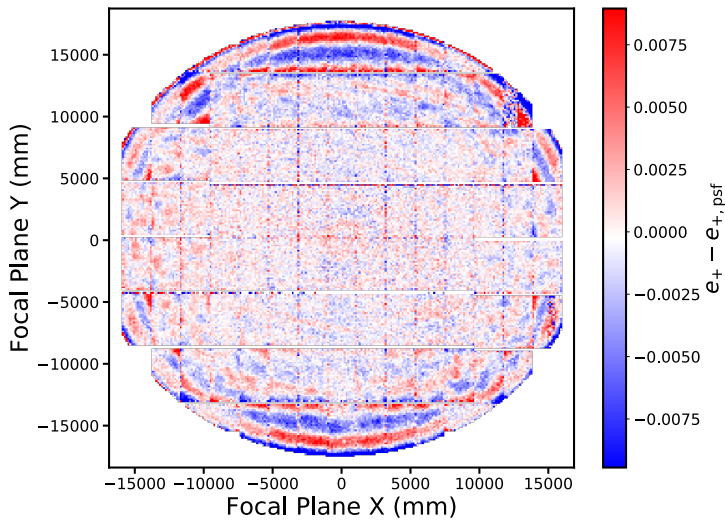
HSC, (Mandelbaum 2018)

PSF model residuals, more examples
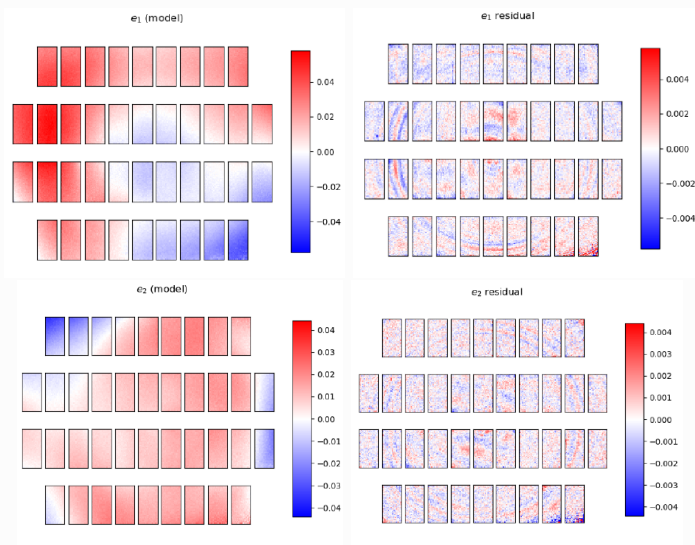

CFIS, from Axel Guinot.

Results from weak-lensing surveys

1. Early era: 2000 - 2006
2. Consolidating era: 2007 – 2012
3. Small-survey era: 2013 – 2016
4. Medium survey era: 2017 – 2021
5. Large survey era: 2022 – 2030

State of the art $\sim$ 2013: CFHTLenS
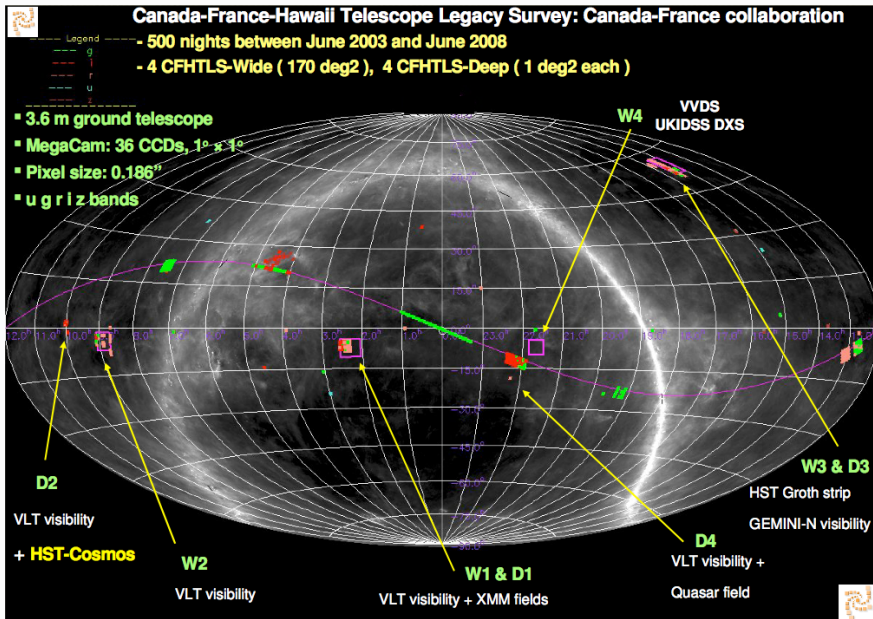
State of the art $\sim$ 2013

CFHTLenS
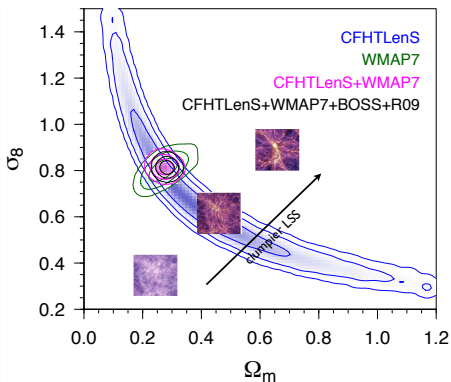
2D lensing
(Kilbinger et al. 2013)

6-bin tomography
(Heymans et al. 2013)

(σ_8: power-spectrum normalisation; RMS of density fluct. in 8 Mpc spheres.)

# Ongoing surveys: KiDS
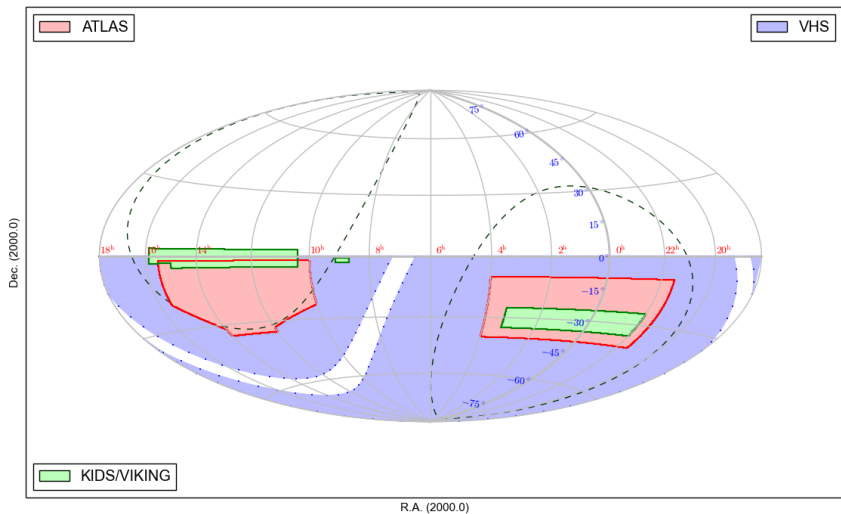
Ongoing surveys: DES
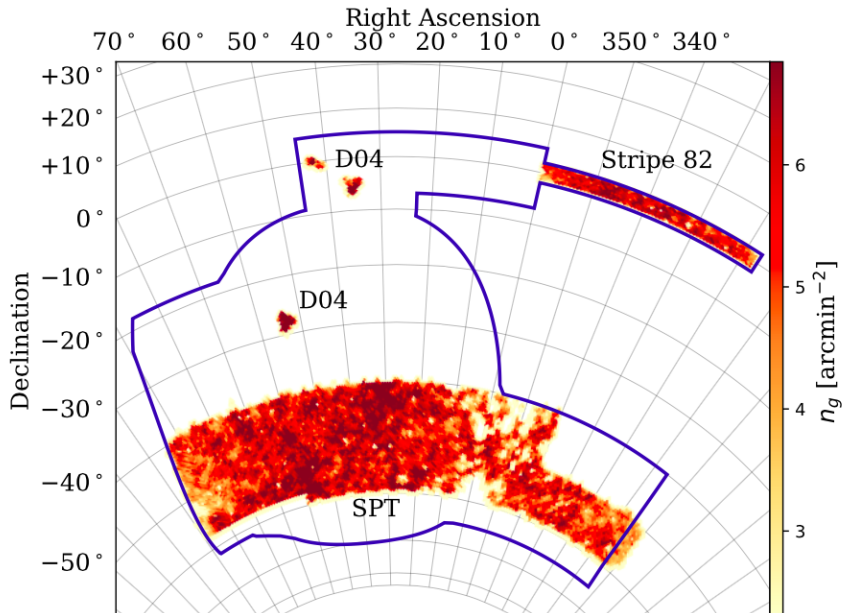
More recent results ~ 2017
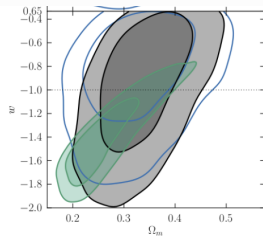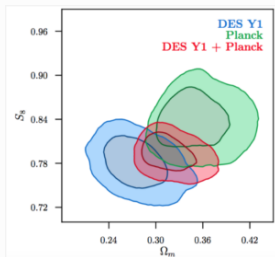
(DES Coll. et al. 2017) - DES WL + GC   (Troxel et al. 2017) - DES
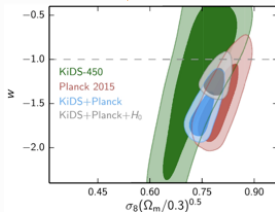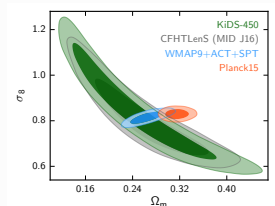
(Hildebrandt et al. 2017) - KiDS   (Joudaki et al. 2017) - KiDS

Discrepancy with Planck? I

- Only 2 - 3σ. However, also discrepancy of CMB C_ℓ's with SZ cluster counts.
- Additional physics, e.g. massive neutrinos? Not sufficient evidence.
- WL systematics? (E.g. shear bias, baryonic uncertainty on small scales.) KiDS say not likely.

Updates

1. Weak-lensing, (Troxel et al. 2018). Improved computation of shape noise, shear bias correction, and angular scales weighting.
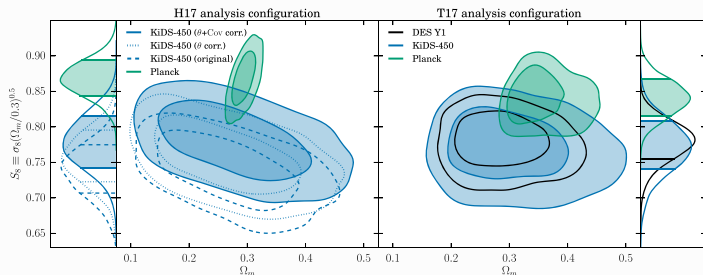
Discrepancy with Planck? II

2. Planck 2018 results, (Planck Collaboration et al. 2018)
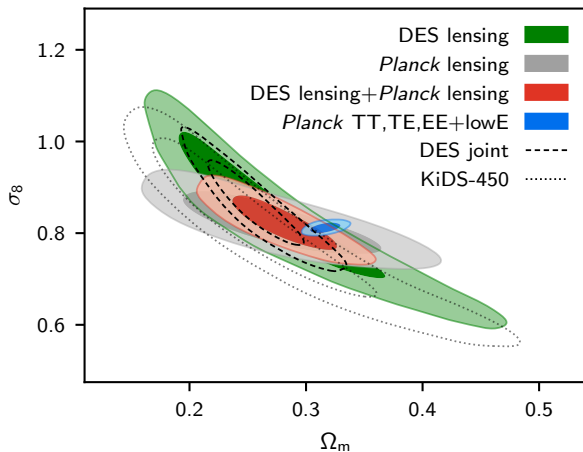
Discrepancy with Planck? III

3. KiDS + DES, redshift calibration.
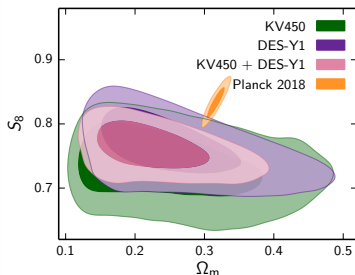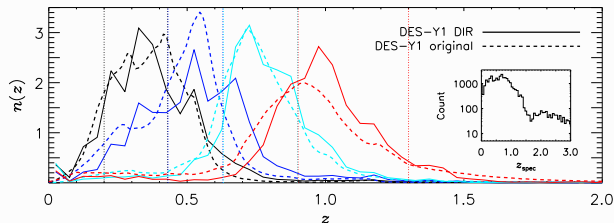
(Joudaki et al. 2019)

ESA Euclid mission:

- Total mass satellite :
  2 200 kg

- Dimensions:
  4,5 m x 3 m

- Launch: end 2020 by a Soyuz rocket from the Kourou space port

Euclid placed in L2

- Survey: 6 years,

Sun shield (Thales Alenia Space)

Telescope
(Airbus Defence and Space)

Service Module (Thales Alenia Space)

VIS+ NISP
(Euclid Consortium)

esa
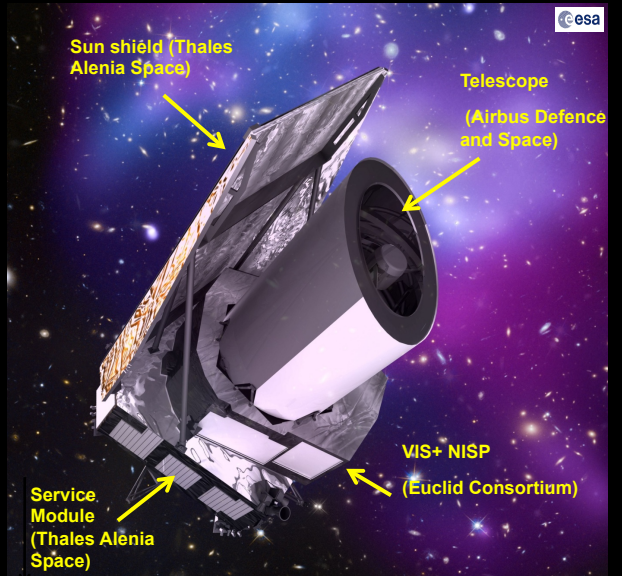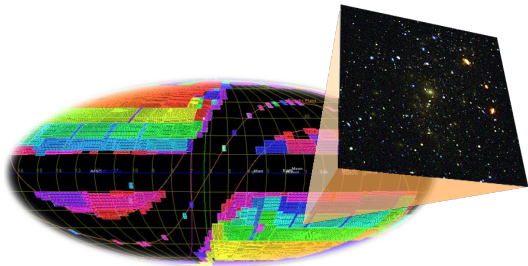
Euclid area = $15,000$ deg^2 (extra-galactic and -ecliptic sky).
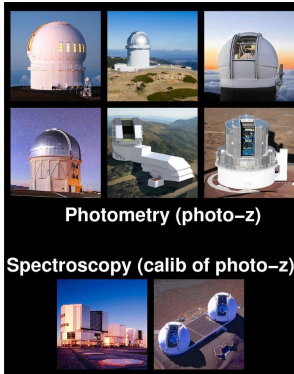
Ground-based observations for photometric redshifts.
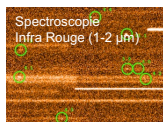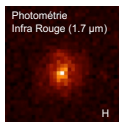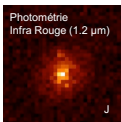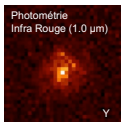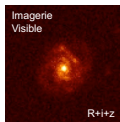
10 billions of galaxies observed in visible and infra red photometry

50 millions of infra red spectra

Euclid imaging and spectroscopy.

Euclid

Two instruments:

- Visible imager, WL, 1.5×10^9 galaxies
- Near-IR imager + spectrograph, 3×10^7 galaxy spectra

Cosmology

- Dark-energy equation of state w to 2% (currently $\sim 20\%$)
- Constrain models of modified gravity
- Neutrino masses to 0.02 eV (currently ~ 0.3 eV)
- Map dark matter distribution
- Early-universe conditions, inflation: limit non-Gaussianity $f_{\rm NL}$ to ± 2 (currently $\sim \pm 6$)

"Legacy"

- High-redshift galaxies, AGN & clusters @ $z > 1$, QSO @ $z > 8$, strong lensing galaxy candidates: Increase of numbers by several orders of magnitude

SLACS (~2010 - HST): gravitational lensing by galaxies

euclid consortium

SDSS J1420+6019	SDSS J2321−0939	SDSS J1106+5228	SDSS J1029+0420	SDSS J1143−0144	SDSS J0955+0101	SDSS J0841+3824	SDSS J0044+0113	SDSS J1432+6317	SDSS J1451−0239
SDSS J0959+0410	SDSS J1032+5322	SDSS J1443+0304	SDSS J1218+0830	SDSS J2238−0754	SDSS J1538+5817	SDSS J1134+6027	SDSS J2303+1422	SDSS J1103+5322	SDSS J1531−0105
SDSS J0912+0029	SDSS J1204+0358	SDSS J1153+4612	SDSS J2341+0000	SDSS J1403+0006	SDSS J0936+0913	SDSS J1023+4230	SDSS J0037−0942	SDSS J1402+6321	SDSS J0728+3835
SDSS J1627−0053	SDSS J1205+4910	SDSS J1142+1001	SDSS J0946+1006	SDSS J1251−0208	SDSS J0029−0055	SDSS J1636+4707	SDSS J2300+0022	SDSS J1250+0523	SDSS J0959+4416
SDSS J0956+5100	SDSS J0822+2652	SDSS J1621+3931	SDSS J1630+4520	SDSS J1112+0826	SDSS J0252+0039	SDSS J1020+1122	SDSS J1430+4105	SDSS J1436−0000	SDSS J0109+1500
SDSS J1416+5136	SDSS J1100+5329	SDSS J0737+3216	SDSS J0216−0813	SDSS J0935−0003	SDSS J0330−0020	SDSS J1525+3327	SDSS J0903+4116	SDSS J0008−0004	SDSS J0157−0056

SLACS: The Sloan Lens ACS Survey   www.SLACS.org

SLACS

Euclid VIS Legacy : after 2 months

(66 months planned)

140,000 strong lenses by galaxies, 5000 giant arcs in clusters

Weak-lensing mass maps @ very high resolution
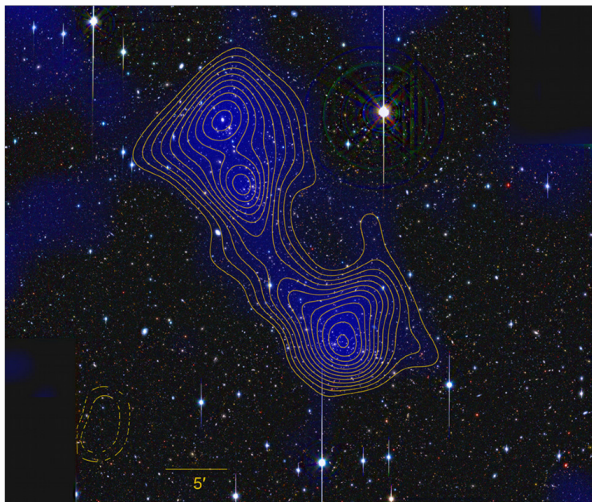
A 222/223, filament between clusters (Dietrich et al. 2012)

Euclid imaging

M51
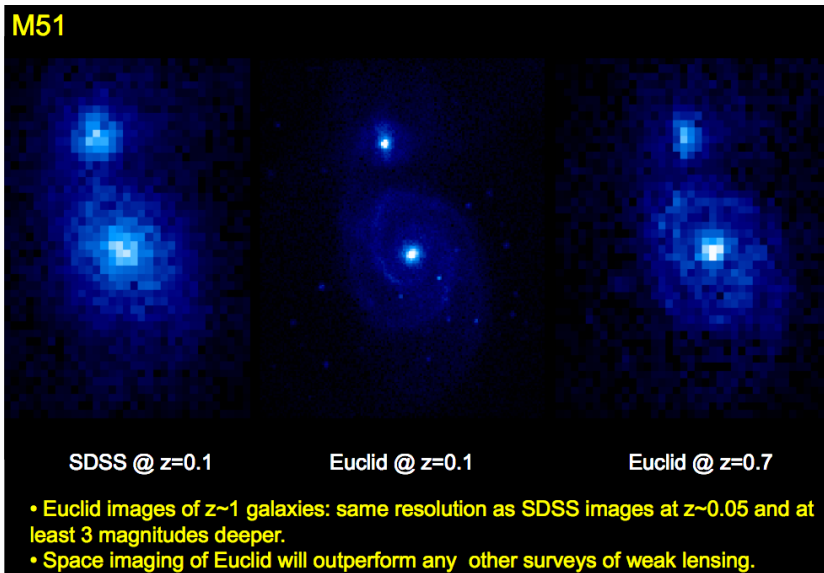
SDSS @ z=0.1   Euclid @ z=0.1   Euclid @ z=0.7

• Euclid images of z~1 galaxies: same resolution as SDSS images at z~0.05 and at least 3 magnitudes deeper.
• Space imaging of Euclid will outperform any other surveys of weak lensing.

Euclid WL challenges

Color gradients

2 galaxy components — color-dependent PSF — convolve — observe simultaneously in broad filter +
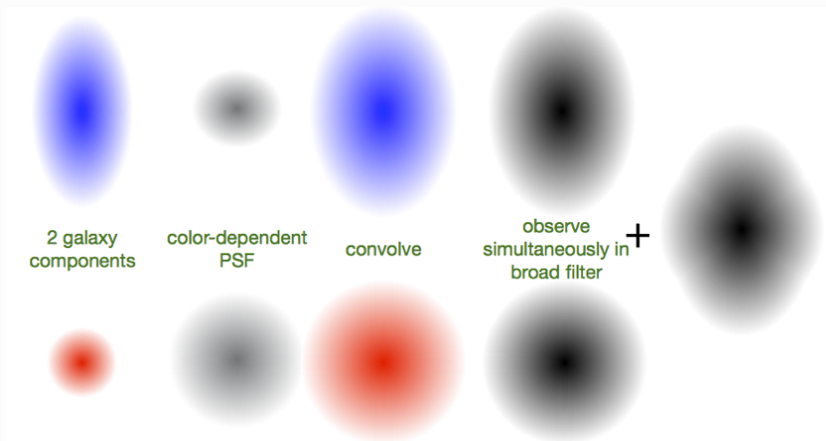
Euclid observes without optical filter (equiv. $R + I + z$). Calibrate color effects using HST multi-band observations.

The bullet cluster and the nature of dark matter

The bullet cluster
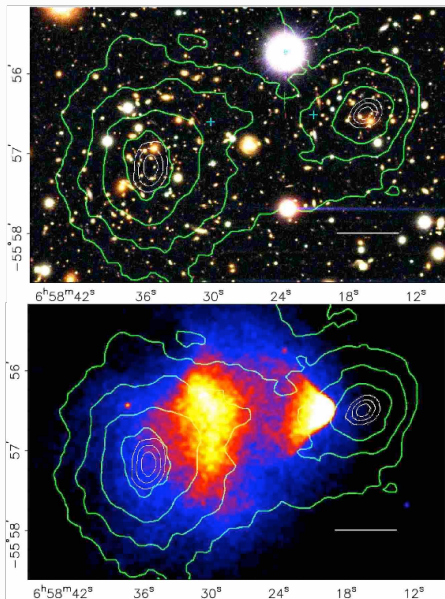
Clowe et al. (2006)

- Merging galaxy cluster at $z = 0.296$
- Recent major merger 100 Myr ago
- Components moving nearly perpendicular to line of sight with $v = 4700$ km s^{-1}
- Galaxy concentration offset from X-ray emission. Bow shocks visible

The bullet cluster: SL+WL measurements

Instrument	Date of Obs.	FoV	Passband	$t_{\rm exp}$ (s)	$m_{\rm lim}$	$n_{\rm d}$ $('^{-2})$	seeing
2.2m ESO/MPG	01/2004	$34' \times 34'$	R	14100	23.9	15	$0''8$
Wide Field Imager	01/2004		B	6580			$1''0$
	01/2004		V	5640			$0''9$
6.5m Magellan	01/15/2004	$8'$ radius	R	10800	25.1	35	$0''6$
IMACS	01/15/2004		B	2700			$0''9$
	01/15/2004		V	2400			$0''8$
HST ACS	10/21/2004	$3'5 \times 3'5$	F814W	4944	27.6	87	$0''12$
subcluster	10/21/2004		F435W	2420			$0''12$
	10/21/2004		F606W	2336			$0''12$
main cluster	10/21/2004	$3'5 \times 3'5$	F606W	2336	26.1	54	$0''12$

(?, ?)

The bullet cluster: strong lensing
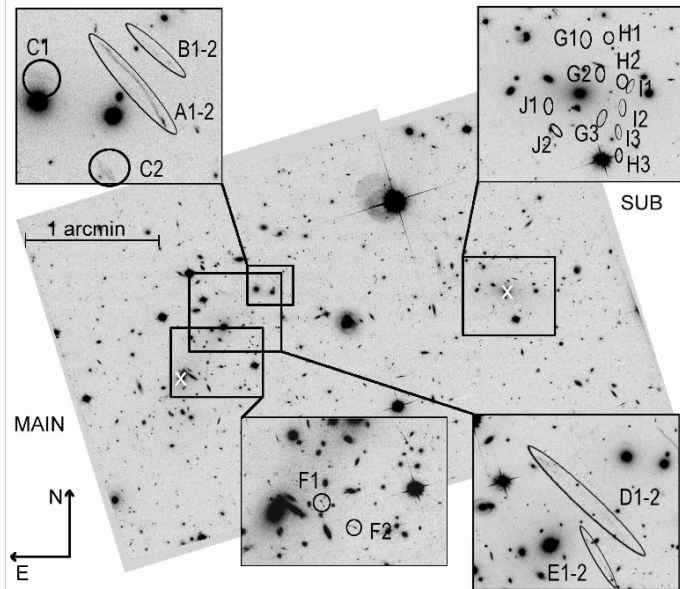
The bullet cluster: WL and X-ray
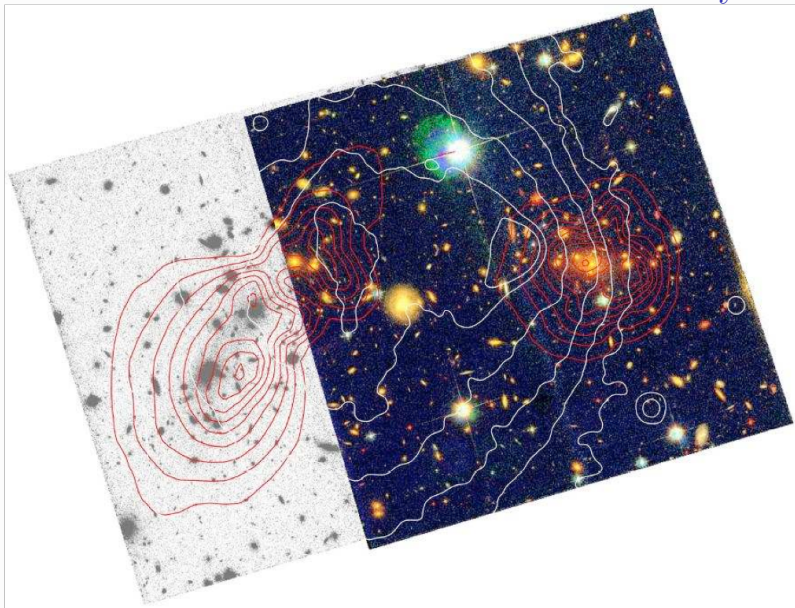
The bullet cluster: Evidence for dark matter

- 10σ (6σ) offset between main (sub-)mass peak and X-ray gas $\rightarrow$ most cluster mass is not in hot X-ray gas (unlike most baryonic mass: $m_X \gg m_*$!)
- Main mass associated with galaxies $\rightarrow$ this matter is collisionless

Modified gravity theories without dark matter: MoND (Modified Newtonian Dynamics), (Milgrom 1983), changes Newton's law for low accelerations ($a \sim 10^{-10}$ m s^{-2}), can produce flat galaxy rotation curves and Tully-Fisher relation.

MoND's relativistic version (Bekenstein 2004), varying gravitational constant $G(r)$. Introduces new vector field ("phion") with coupling strenght $\alpha(r)$ and range $\lambda(r)$ as free functions.

This can produce non-local weak-lensing convergence mass, where $\kappa \not\propto \delta$! Necessary to explain offset between main κ peak and main baryonic mass. Model with four mass peaks can roughly reproduce WL map with additional collisionless mass! E.g. 2 eV neutrinos.

The bullet cluster: MoND model
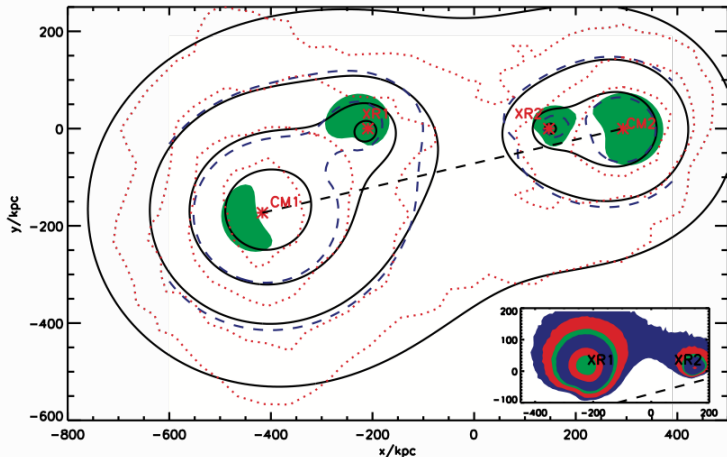
FIG. 1.— Our fitted convergence map (solid black lines) overplotted on the convergence map of C06 (dotted red lines) with x and y axes in kpc. The contours are from the outside 0.16, 0.23, 0.3 and 0.37. The centres of the four potentials we used are the red stars which are labelled. Also overplotted (blue dashed line) are two contours of surface density [4.8 & 7.2]$\times 10^2 M_\odot$ pc^{-2} for the MOND standard μ function; note slight distortions compared to the contours of κ. The green shaded region is where matter density is above $1.8 \times 10^{-3} M_\odot$ pc^{-3} and correspond to the clustering of 2eV neutrinos. *Inset:* The surface density of the gas in the bullet cluster predicted by our collisionless matter subtraction method for the standard μ-function. The contour levels are [30, 50, 80, 100, 200, 300]$M_\odot pc^{-2}$. The origin in RA and dec is $[06^h 58^m 24.38^s, -55^o 56'.32]$

Bibliography I

Bekenstein J D 2004 *Phys. Rev. D* **70**(8), 083509.

DES Coll., Abbott T M C, Abdalla F B, Alarcon A, Aleksić J & al. 2017 *arXiv* **1708.01530**.

Einstein A 1915 *Sitzungsberichte der Königlich Preußischen Akademie der Wissenschaften (Berlin), Seite 844-847.* .

Gentile M, Courbin F & Meylan G 2013 *A&A* **549**, A1.

Heymans C, Grocutt E, Heavens A, Kilbinger M, Kitching T D & al. 2013 *MNRAS* **432**, 2433–2453.

Hildebrandt H, Viola M, Heymans C, Joudaki S, Kuijken K & al. 2017 *MNRAS* **465**, 1454–1498.

Jarvis M, Sheldon E, Zuntz J, Kacprzak T, Bridle S L & al. 2016 *MNRAS* **460**, 2245–2281.

Joudaki S, Hildebrandt H, Traykova D, Chisari N E, Heymans C & al. 2019 *arXiv e-prints* p. arXiv:1906.09262.

Joudaki S, Mead A, Blake C, Choi A, de Jong J & al. 2017 *MNRAS* **471**, 1259–1279.

Bibliography II

Kilbinger M, Fu L, Heymans C, Simpson F, Benjamin J & al. 2013 *MNRAS* **430**, 2200–2220.

Mandelbaum R 2018 *ARA&A* **56**, 393–433.

Milgrom M 1983 *Astrophysical Journal* **270**, 371–389.

Ngolè Mboula F M, Starck J L, Okumura K, Amiaux J & Hudelot P 2016 *ArXiv e-prints* .

Planck Collaboration, Aghanim N, Akrami Y, Ashdown M, Aumont J & al. 2018 *ArXiv e-prints* .

Potter D, Stadel J & Teyssier R 2016 *ArXiv e-prints* .

Springel V, White S D M, Jenkins A, Frenk C S, Yoshida N & al. 2005 *Nature* **435**, 629–636.

Troxel M A, Krause E, Chang C, Eifler T F, Friedrich O & al. 2018 *MNRAS* **479**, 4998–5004.

Troxel M A, MacCrann N, Zuntz J, Eifler T F, Krause E & al. 2017 *arXiv* **1708.01538**.

Walsh D, Carswell R F & Weymann R J 1979 *Nature* **279**, 381–384.

Bibliography III

Zuntz J, Sheldon E, Samuroff S, Troxel M A, Jarvis M & al. 2018 *MNRAS*
481, 1149–1182.